



OPEN

## Flavonolignans silybin, silychristin and 2,3-dehydrosilybin showed differential cytoprotective, antioxidant and anti-apoptotic effects on splenocytes from Balb/c mice

Zuzana Jurčáková<sup>1</sup>, Gabriela Hrčková<sup>1</sup>  , Dagmar Mudroňová<sup>2</sup>, Anna Alexovič Matiašová<sup>3</sup> & David Biedermann<sup>4</sup>

Silymarin is an extract obtained from the seeds of milk thistle (*Silybum marianum* L., Asteraceae) and contains several structurally related flavonolignans and a small family of flavonoids. Mouse spleen cells represent highly sensitive primary cells suitable for studying the pharmacological potential and biofunctional properties of natural substances. Cultivation of splenocytes for 24 h under standard culture conditions (humidity, 37 °C, 5% CO<sub>2</sub>, atmospheric oxygen) resulted in decreased viability of splenocytes compared to intact cells. A cytoprotective effect of silybin (SB), silychristin (SCH) and 2,3-dehydrosilybin (DHSB) was observed at concentrations as low as 5 μmol/ml. At 50 μmol/ml, these substances restored and/or stimulated viability and mitochondrial membrane potential and had anti-apoptotic effect in the order SB > DHSB > SCH. The substances demonstrated a concentration-dependent activity in restoring the redox balance based on the changes in the concentration of reactive oxygen species (ROS), hydrogen peroxide (H<sub>2</sub>O<sub>2</sub>) and nitric oxide. This was in the order DHSB > SCH > SB, which correlated with the suppressed expression of nuclear factor erythroid 2-related factor 2 (Nrf2), catalase and glutathione peroxidase. The strong stimulation of the superoxide dismutase 1 gene converting ROS to H<sub>2</sub>O<sub>2</sub> points to its dominant role in the maintaining redox homeostasis in splenocytes, which was disrupted by oxidative stress due to non-physiological culture conditions. Our study showed significant differences in the cytoprotective, antioxidant and anti-apoptotic activities of SB, SCH, and DHSB on splenocytes exposed to mild and AAPH-induced oxidative stress.

**Keywords** Mouse splenocytes, Silybin, Silychristin, 2,3-dehydrosilybin, Redox balance, Viability, Apoptosis

Polyphenols are a wide group of natural compounds which are probably the most commonly represented natural compounds in the human diet. Among them, flavonoids are compounds present in plants characterized by typical 6-3-6 carbon structural motive. Silymarin is the extract obtained from the seeds of the milk thistle plant (*Silybum marianum* L., Asteraceae) and contains several structurally related flavonolignans, representing approximately 95% of the extract<sup>1,2</sup>. Silymarin is traditionally used as supportive therapy for liver diseases and numerous studies have demonstrated anticancer, hypocholesterolemic, cardioprotective and also immunomodulatory activities<sup>3-5</sup>. The well-documented antioxidant capacity of silymarin contributed to the improvement of pathological manifestations in many diseases. The individual components of silymarin, namely the most abundant flavonolignans, participate specifically in its final effects described above. Silybin (SB) as a major bioactive component of silymarin is the best studied<sup>6,7</sup>. Gu et al.<sup>8</sup> exposed mice to a hyperlipidic diet to

<sup>1</sup>Institute of Parasitology, Slovak Academy of Sciences, Hlinkova 3, 04001 Kosice, Slovakia. <sup>2</sup>Department of Microbiology and Immunology, University of Veterinary Medicine and Pharmacy, Kosice, Slovakia. <sup>3</sup>Institute of Biology and Ecology, Faculty of Science, P. J. Šafárik University, Kosice, Slovakia. <sup>4</sup>Institute of Microbiology, Academy of Sciences of the Czech Republic, Prague, Czech Republic.  email: hrcka@saske.sk

induce obesity, insulin resistance, hyperlipidemia, and hepatic steatosis. The results showed that SB significantly contributed to the normalisation this metabolic syndrome. SB is also a potent antineoplastic compound which was demonstrated in in vitro studies on various types of cancer<sup>9</sup> and others. SB also has radioprotective properties that can prevent DNA damage caused by gamma radiation<sup>10,11</sup> and photoprotective effects against UVA radiation from sunlight<sup>12</sup>. Silychristin (SCH), like many components of the extract, exhibits antioxidant properties and other biological properties, for example, inhibition of  $\alpha$ -glucosidase and stimulation of insulin secretion in rats with type I diabetes mellitus<sup>13</sup>. Bijak et al.<sup>14</sup> described significant concentration-dependent anti-inflammatory effects of SCH. The oxidized derivative of silybin—2,3-dehydrosilybin (DHSB) occurs in the extract in small but non-negligible amounts (up to 3%)<sup>1</sup>. Due to the presence of a 2,3-double bond in DHSB, it has a significantly higher antioxidant capacity, which leads to up to 25 times better capture of free radicals, as well as several times better inhibition of lipid peroxidation compared to SB<sup>15,16</sup>. DHSB also shows promising results in anti-inflammatory and anti-fibrotic therapies<sup>14</sup> and the prevention of chronic liver damage<sup>17</sup>. Immune cells such as lymphocytes, macrophages and dendritic cells are particularly sensitive to the changes in the levels of free oxygen and nitrogen radicals, which play an important role in inflammatory processes and pathogenesis of many diseases<sup>18</sup>. Reactive oxygen species (ROS) are produced in the cells during normal metabolism and play vital roles in the stimulation of signaling pathways in response to the changes in intra- and extracellular conditions. However, when ROS are produced over a long time at higher concentrations, significant damage to the cell structure and functions occurs<sup>19</sup>.

There is a limited amount of information about the effects of individual flavonolignans on immune cells. In our work, we, therefore, focused on evaluating the antioxidant, cytoprotective and anti-apoptotic effects of SB, SCH and DHSB on the spleen cells isolated from healthy Balb/c mice by monitoring viability, changes in mitochondrial activity and apoptosis as well as the effect of substances on the production of free oxygen and nitrogen radicals,  $H_2O_2$  and changes in the expression of selected genes with a role in endogenous antioxidant mechanisms.

## Material and methods

### Preparation of flavonolignans

Silymarin was purchased from Liaoning Senrong Pharmaceutical Co., Ltd. (Liaoning, China). The silymarin flavonolignans were prepared as described before<sup>20</sup> at the Institute of Microbiology of the CAS, v. v. i. Briefly, the silybin (diastereomeric mixture of A + B) was isolated by suspending the silymarin in methanol and after a short stirring the insoluble silybin was filtered off. SCH (a natural mixture of diastereomers A/B 95:5) was isolated from the black residue by LH-20 column chromatography<sup>20</sup>. DHSB (racemate) was prepared by iodine oxidation from silybin with a purity of more than 95%<sup>21</sup>. The stock solutions of flavonolignans were prepared in DMSO.

### Experimental design, isolation and cultivation of mouse splenic cells

We focussed on how the selected silymarin flavonolignans depending on their concentration, can affect the vital functions of splenocytes after 24 h incubation under standard cultivation conditions (5%  $CO_2$ , humidity and access to atmospheric oxygen ~ 19–21%). In addition, oxidative stress in the cells was induced using 2,2'-azobis(2-amidinopropane) dihydrochloride (AAPH, 5  $\mu$ l/ml) for 1 h before the end of incubation in tests aimed at monitoring changes in the level of ROS,  $H_2O_2$  and NO. Experiments were performed on 8-week-old, healthy, male Balb/c mice bred at the Institute of Parasitology in the animal facilities. The animals were killed humanely with sodium pentobarbital, a euthanasia preparation at a dose of 86 mg/kg body weight, intraperitoneally with subsequent cervical dislocation. A total of eight in vitro experiments were performed, in which the spleens of three mice were aseptically isolated. The splenocyte suspensions were resuspended in cold RPMI 1640 medium (Biochrom-Merck, Germany) containing 2 mM of stable glutamine, 10% heat-inactivated bovine foetal serum (Biochrom-Merck, Berlin, Germany), 100 U/ml of penicillin, 100  $\mu$ g/ml of streptomycin, 10  $\mu$ g/ml of gentamicin and 2.5  $\mu$ g/ml of amphotericin B (all from Sigma-Aldrich, St. Louis, MO, USA). Red blood cells were removed by incubating the suspensions with lysis solution. The viability of splenocytes from each mouse was assessed by trypan blue exclusion assay and was greater than 97% of the total number counted.

### Viability test—trypan blue absorption

Splenocyte suspensions diluted to a concentration of  $1 \times 10^6$  cells/ml in culture medium were added in triplicate to CultureSlides (Falcon Tissue Culture Treated Glass Slides, Corning, NY, USA) for each treatment and solutions of individual flavonolignans (SB, SCH, DHSB) were added to the cells to reach the final concentrations of 5 and 50  $\mu$ mol/ml. Untreated splenocytes were used as controls. After 24 h of incubation, non-adherent cells were collected and the proportions (%) of live (white) and dead (blue) cells from a total of 300 cells were counted after the addition of trypan blue. The viability of cells adherent to the slide was counted in a similar manner, and then the proportions of live cells in both cell populations were summed and expressed as mean  $\pm$  SD. Viability was assessed in two independent in vitro experiments.

### MTT test

Splenocyte suspensions diluted to a concentration of  $1 \times 10^6$  cells/ml in culture medium were incubated in 24-well plates in triplicate for each treatment and control. Splenocytes were cultured for 24 h with SB, SCH and DHSB at concentrations of 5 or 50  $\mu$ mol/ml. MTT (5 mg/ml in PBS) was added 4 h before the end of the assay. Cell pellets containing formazan crystals were dissolved in 100  $\mu$ l of dimethyl sulfoxide (DMSO) and absorbance was measured at 550 nm with a reference filter at 630 nm using a Multiscan FC Plate Reader (Thermo Scientific, Finland). Optical density (OD) values for adherent and non-adherent cells/samples were summed and used to calculate the mean and standard deviation ( $\pm$  SD) of the three repeated in vitro experiments.

### Neutral red uptake assay

The neutral red uptake assay is another test for assessing cell viability<sup>22</sup>. Splenocyte suspensions ( $1 \times 10^6$  cells/ml) were incubated in 24-well plates in triplicate for untreated control and cells treated with SB, SCH and DHSB at concentrations of 5 or 50  $\mu\text{mol}/\text{ml}$  for 24 h. One hour before the end of the test, 20  $\mu\text{g}$  of neutral red was added to each well. Extraction of internalized dye was performed separately for non-adherent and adherent cell populations using 200  $\mu\text{l}$  of extraction buffer. The optical density of the extracts for adherent and non-adherent cells was measured in a 96-well plate at 550 nm using a Multiscan FC Plate Reader. The values for both populations were summed and used to calculate the mean  $\pm$  SD from two repeated *in vitro* experiments.

### Mitochondrial membrane potential

Mitochondria are key organelles for survival of cells and change in mitochondrial membrane potential ( $\Delta\psi_m$ ) is defined as an indicator of mitochondrial activity. Splenocytes diluted to the concentration of  $1 \times 10^6$  cells/ml in the culture medium were incubated with 5 or 50  $\mu\text{mol}/\text{ml}$  SB, SCH and 2,3-DHSB for 24 h in 24-well plates. Untreated cells were used as control and mitochondrial potential was assessed also in freshly isolated (intact) cells. Mitochondrial membrane potential was determined by flow cytometry using the fluorescent dye rhodamine 123, which is absorbed by the mitochondria of living cells. Changes in dye absorption reflect  $\Delta\psi_m$  and are expressed as mean fluorescence intensity/cell (MFI). Non-adherent splenocytes were transferred to tubes and adherent cells were detached using 300  $\mu\text{l}$  warm Accutase solution (BioLegend, USA) and washed. Both cell fractions/well were pooled and rhodamine 123 solution was added to the cells at the final concentration of 10  $\mu\text{M}$ . Splenocytes were incubated at 37 °C for 20 min. Mitochondrial membrane potential in the cell suspensions was measured after excitation at 505 nm and emission at 535 nm. The test was repeated two times.

### Annexin V/propidium iodide apoptosis assay

Splenocytes diluted at the concentration of  $1 \times 10^6$  cells/ml were incubated in 24-well plates for 24 h with 5 or 50  $\mu\text{mol}/\text{ml}$  of SB, SCH and DHSB in triplicate; untreated cells were used as control. Freshly isolated cells were used as an intact control. Splenocytes were processed as described previously. Both cell fractions/well were pooled, washed and stained with fluorescent dyes Annexin V and propidium iodide using a kit (BD Pharmingen Annexin V-FITC, BD Biosciences, California, USA). The proportions (%) of live cells and cells in the different stages of apoptosis were analysed by flow cytometry using a FACS Canto flow cytometer. Data were evaluated using FACS Diva software. The test was performed two times.

### Immunofluorescent labelling

The apoptosis in splenocytes was further evaluated by staining of mitochondrial membrane protein B-cell lymphoma-extra large (Bcl-xL, anti-apoptotic). Cells were cultured on Tissue Culture Treated Glass Slides (Falcon, Corning Brand, County Route, NY, USA) for 24 h. Cells were fixed in 4% paraformaldehyde and used for immunofluorescent detection of proteins via fluorescent microscopy. After permeabilization with 0.5% Triton X-100 in PBS and blocking with 2% BSA, cells were incubated with primary antibody against Bcl-xL (mouse monoclonal IgG, purified) (1:100) (Santa Cruz Biotechnology, USA) overnight at 4 °C and then with the secondary antibody rabbit anti-mouse IgG –FITC (1:500) (Abcam, Cambridge, UK). Nuclei were stained with Draq5 dye (1:500) (Abcam, Cambridge, UK) and slides were mounted into ProLong <sup>®</sup>Gold Antifade Reagent (Cell Signaling Technology, MA, USA). Images were obtained using a Leica TCS SP5X confocal microscope and LAS AF software (Leica Microsystems, Mannheim, Germany).

### Determination of intracellular reactive oxygen species

Approximately 90% of cellular oxygen species are generated by mitochondria from aerobic respiration<sup>23</sup>. Splenocytes diluted at the concentration of  $1 \times 10^6$  cells/ml were treated in 24-well plates for 24 h in triplicate with 5 or 50  $\mu\text{mol}/\text{ml}$  of SB, SCH and DHSB. The fluorescent dye H<sub>2</sub>DCFDA was used to determine the production of intracellular ROS. H<sub>2</sub>DCFDA (1 mM, 10  $\mu\text{l}$ ) was added to the cells 4 h before the end of the assay. Oxidative stress was induced using AAPH (5  $\mu\text{l}/\text{ml}$ , 1 mM stock solution), which was added 1 h before the end of the assay. Non-adherent splenocytes were transferred to tubes and adherent cells were detached as described previously. Subsequently, both cell fractions were combined and ROS concentration expressed as MFI and the proportion of ROS-producing cells (%) were evaluated by flow cytometry using a FACS Canto flow cytometer and evaluated using FACS Diva software. The test was repeated twice.

### Determination of extracellular hydrogen peroxide production

To determine extracellular production of hydrogen peroxide (H<sub>2</sub>O<sub>2</sub>) a modified method of Santos et al.<sup>24</sup> was used. The principle of the method is the oxidation of phenol red dye by H<sub>2</sub>O<sub>2</sub> under the catalytic activity of the added horseradish peroxidase II (HRP II) enzyme. Splenocytes ( $1 \times 10^6$  cells/ml) were diluted in Hanks' balanced salt solution (HBSS) without phenol red, which was added at a final concentration of 0.55 mM and supplemented with 10  $\mu\text{g}/\text{ml}$  HRP II. Cells were cultured in a 96-well plate ( $2 \times 10^5/\text{well}/200 \mu\text{l}$ ) in triplicate for each group and treated with 5 or 50  $\mu\text{mol}/\text{ml}$  of SB, SCH and DHSB for 2 h. The reaction was stopped with 10  $\mu\text{l}$  of 2N NaOH. Optical density was measured at 620 nm using a Multiscan FC Plate Reader and H<sub>2</sub>O<sub>2</sub> concentrations (in  $\mu\text{M}$ ) were calculated based on a calibration curve. The test was performed twice.

### Determination of nitric oxide (NO) with the Griess reagent

Splenocytes at the concentration of  $1 \times 10^6$  cells/ml in the RPMI medium were treated with 5 or 50  $\mu\text{mol}/\text{ml}$  flavonolignans in 24-well plates for 24 h in duplicate. Freshly isolated cells were used as an intact control. AAPH was added to the cells one hour before the end of the assays. The concentration of NO in the supernatants was measured as nitrite (NO<sub>2</sub><sup>-</sup>) using Griess reagent (Sigma-Aldrich, USA) by the protocol described previously<sup>25</sup>.

Absorbance was measured at 550 nm using a Multiscan FC Plate Reader. Nitrite concentration was determined using a calibration curve with 0.1 M NaNO<sub>3</sub> as standard. The test was carried out twice.

### RNA isolation from cells, cDNA synthesis and gene expression analysis using quantitative PCR

Splenic cells ( $1 \times 10^6$ /ml) were incubated in a 24-well plate in triplicate/group and treated with 5 or 50  $\mu\text{mol}/\text{ml}$  of SB, SCH and DHSB. Non-adherent cells were harvested and transferred to TRIzol RNA Isolation Reagent (Invitrogen, Carlsbad, CA, USA). Adherent cells were immersed in TRIzol reagent and both cell fractions were pooled and used for RNA extraction. Isolated RNA was quantified using an AstraGene NanoSpectrophotometer (Harston, Cambridge, UK) and 2  $\mu\text{g}$  was transcribed into cDNA using 1  $\mu\text{l}$  oligo(dT)18 primer (100 pmol/ $\mu\text{l}$ ) 0.3 M dithiothreitol (DTT), 10 mM dNTP mix, 20 U of RNase inhibitor and the reverse transcriptase enzyme RevertAid H Minus (200 U) (all from ThermoFisher Scientific, USA). The cDNA from each sample was used as a template for qPCR.

Quantitative PCR (qPCR) analysis of the relative amount of mRNA was performed using BioRad CFX thermocycler (BioRad, USA). The qPCR reaction mixture (20  $\mu\text{l}$ ) contained 10  $\mu\text{l}$  iQ™ SYBR Green master mix, 1  $\mu\text{l}$  of each primer pair (10 pmol/ $\mu\text{l}$ ), 2  $\mu\text{l}$  cDNA from each sample and 6  $\mu\text{l}$  DEPC-treated water. The specificity of the reaction with each primer pair was tested using a negative control. The pairs of primers used for gene expression analysis are shown in Supplementary Table 1. The melting curves of the product were monitored. Cycle threshold (C<sub>t</sub>) values were normalized to the housekeeping gene Glyceraldehyde 3-phosphate dehydrogenase (GAPDH). Relative gene expression was calculated using the  $2^{-\Delta\Delta\text{Ct}}$  method<sup>26</sup> using intact cell data as a calibration value.

### Statistical analysis

Statistical analysis of the obtained data was performed using GraphPad Prism (version 10) for Windows (GraphPad Software, Inc., San Diego, CA, USA), and the results were expressed as mean  $\pm$  standard deviation calculated from three samples/group of two or three independent in vitro experiments. Results were analysed either by one-way analysis of variance (ANOVA) followed by Tukey's post hoc test or by two-way ANOVA and Sidak's post hoc test. Statistically significant differences compared to the control or intact group are indicated as \* $p < 0.05$ , \*\* $p < 0.01$ , \*\*\* $p < 0.001$ .

### Ethical approval

All experimental procedures and methods were carried out in accordance with guidelines laid down by Government Regulation, § 35, no. 377/2012 Coll., establishing requirements for the protection of animals used for scientific purposes or educational purposes as amended by SR Government Regulation No. 199/2019 Coll. All methods are reported per ARRIVE guidelines. The study procedures were approved by the Ethics Committee of the State Veterinary and Food Administration of the Slovak Republic under protocol No. 3871/15-221d.

## Results

### Effects of silybin, silychristin and 2,3-dehydrosilybin on splenocyte viability

The concentration-dependent effect of selected silymarin flavonolignans on the viability of splenocytes incubated in a complete RPMI medium was evaluated using three standard tests, each reflecting a different physiological process in the cells. The viability of freshly isolated splenocytes (intact) was compared with untreated cells after 24 h of incubation (Ctrl).

The standard culture conditions resulted in a significantly reduced number of live splenocytes assessed by Trypan blue assay ( $71.90 \pm 2.1$ ,  $p < 0.001$ , Fig. 1a). The percentage of viable cells cultured with SB, SCH and DHSB increased at both monitored concentrations (5 and 50  $\mu\text{mol}/\text{ml}$ ) ( $p < 0.001$ ) in comparison with Ctrl group. However, it did not reach values in the intact group. The most potent cytoprotective effect was observed in culture treated with 50  $\mu\text{mol}/\text{ml}$  of SB followed by 50  $\mu\text{mol}/\text{ml}$  of DHSB which was reflected by the highest proportions of live cells ( $91.63 \pm 3.5\%$  and  $87.17 \pm 2.3\%$  resp.)

The impact of SB, SCH and DHSB on cell viability was also evaluated using the MTT test. Compared to intact freshly isolated cells, the values in control cells decreased to  $75.21 \pm 5.5\%$  ( $p < 0.001$ , Fig. 1b) after 24 h of incubation and restoration of viability was found in all groups, most pronounced after treatment with SB ( $112.68 \pm 4.3\%$ ) and DHSB ( $109.39 \pm 2.3\%$ ) ( $p < 0.001$ ) at a concentration of 50  $\mu\text{mol}/\text{ml}$ . Splenocyte viability was also assessed using the neutral red absorption assay. Similarly, as in the previous assays, the proportions of cells actively absorbing dye were significantly decreased in control cells ( $86.01 \pm 3.7\%$ ) compared to freshly isolated splenocytes ( $p < 0.001$ ) and elevated in all groups (Fig. 1c). In the case of lower concentrations of flavonolignans, neutral red uptake was significantly increased in the presence of DHSB ( $p < 0.05$ ). The higher concentration resulted in significantly more intense uptake for all three substances, the most after SB ( $114.23 \pm 4.1$ ). Incubation of the splenocytes alone and in combination with AAPH (1 mM, 5  $\mu\text{l}$ ) did not significantly affect their viability in the mentioned tests, and for this reason, the results are not shown in the given study.

### Effects of silybin, silychristin and 2,3-dehydrosilybin on intracellular ROS production

Intracellular ROS levels were determined using the fluorescent dye H<sub>2</sub>DCFDA. Compared to intact cells, the percentage of ROS-producing cells was reduced after 24 h incubation, which was reversed after the addition of AAPH. In all groups treated with flavonolignans alone and in combination with AAPH, an average of  $99.5\% \pm 0.3$  cells produced ROS (not shown). Compared to the control, a 5  $\mu\text{mol}/\text{ml}$  concentration of SB significantly increased MFI levels ( $8.54 \pm 0.4 \times 10^3$ ), which were similar to those in the intact group. However, a decline in MFI levels ( $p < 0.001$ ) was recorded after incubation with 50  $\mu\text{mol}/\text{ml}$  of SCH and DHSB (Fig. 2a). Addition of AAPH to the cells stimulated ROS production by splenocytes (Fig. 2b) and strong radical-scavenging ability of

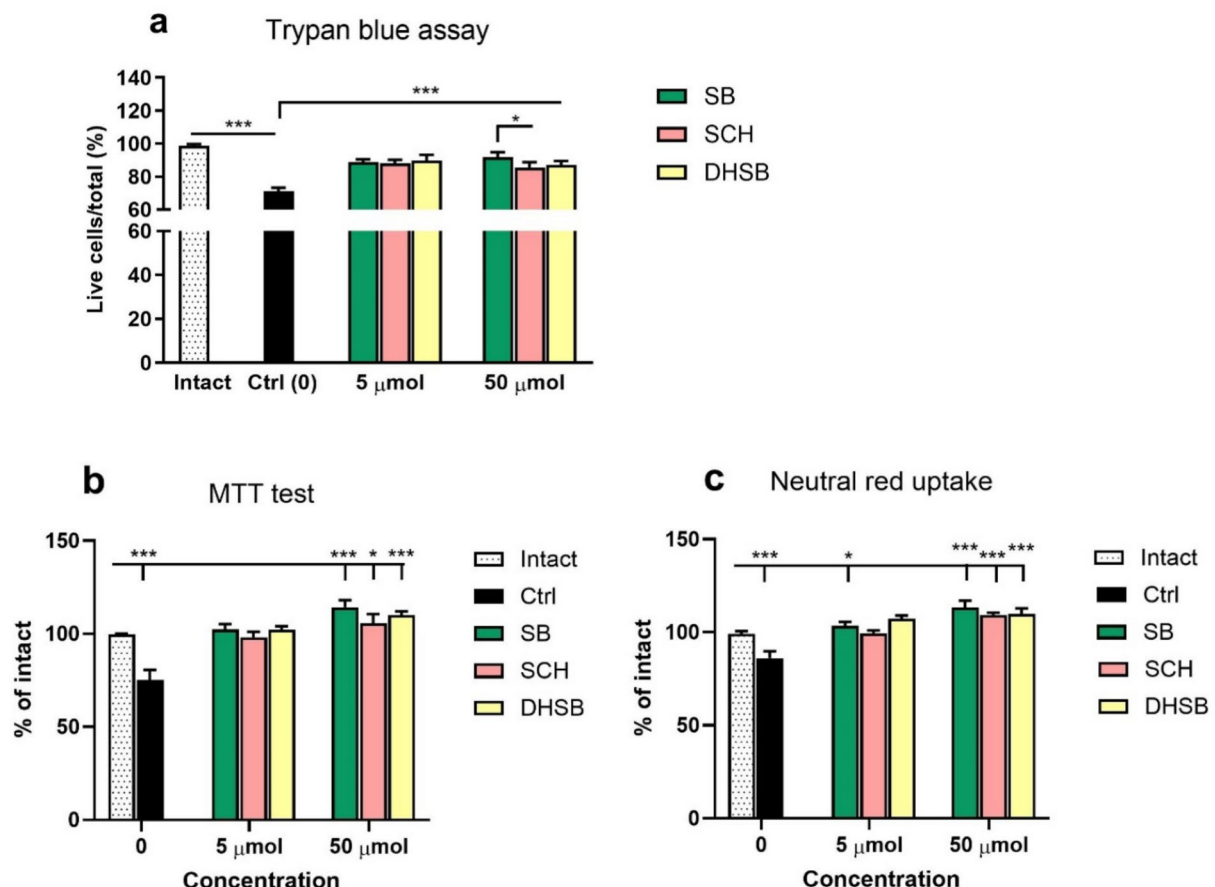


**Fig. 1.** The effects of silybin (SB), silychristin (SCH) and 2,3-dehydrosilybin (DHSB) at 5 and 50  $\mu\text{mol}/\text{ml}$  concentrations on splenocyte viability assessed by: (a) trypan blue exclusion assay, (b, c) MTT assay and (d, e) neutral red absorption assay in intact cells and cells after 24 h incubation (Ctrl). The decrease in viable cells in the control group was calculated as the percentage of viable intact cells (100%) and their proportions after treatment with SB, SCH and DHSB was calculated as percentage of control. Significantly different values between groups are indicated by lines and are marked as: \* $p < 0.05$ , \*\* $p < 0.01$ , \*\*\* $p < 0.001$ , ns—not significant.

flavonolignans at both concentrations was demonstrated by a significant decline of MFI levels ( $p < 0.001$ ), more so at 50  $\mu\text{mol}/\text{ml}$  concentration in the order DHSB > SCH > SB. Representative histograms for selected groups are shown in Fig. 2c.

#### Effects of silybin, silychristin and 2,3-dehydrosilybin on extracellular production of hydrogen peroxide

The extracellular  $\text{H}_2\text{O}_2$  production after incubation in HBSS solution for 2 h (Fig. 3a–b) was significantly increased in cells treated with SB, SCH, and DHSB at concentrations of 5 and 50  $\mu\text{mol}/\text{ml}$  compared to control splenocytes ( $p < 0.001$ ). At both concentrations, higher amounts of  $\text{H}_2\text{O}_2$  were recorded after SCH and DHSB in comparison with SB. After the addition of AAPH, extracellular  $\text{H}_2\text{O}_2$  was increased in all groups, the most after SCH at 5 and 50  $\mu\text{mol}/\text{ml}$  concentrations.

#### Effects of silybin, silychristin and 2,3-dehydrosilybin on nitric oxide (NO) production

NO production was determined in the supernatants of unstimulated spleen cells incubated for 24 h indirectly, by measuring nitrite ( $\text{NO}_2^-$ ) using Griess reagent. Treatment of cells with SB, SCH, and DHSB at both concentrations resulted in significantly higher levels of NO ( $p < 0.001$ ) (Fig. 4a) in comparison with control. Whereas the low concentration had a similar effect, at high concentration a decrease was seen after SB ( $3.75 \pm 0.05 \mu\text{mol}/\text{ml}$ ) in comparison with DHSB ( $4.41 \pm 0.13 \mu\text{mol}/\text{ml}$ ) ( $p < 0.01$ ). The addition of AAPH to the cell suspensions treated with SB, SCH, and DHSB at 5  $\mu\text{mol}/\text{ml}$  concentrations (Fig. 4b) did not stimulate further NO synthesis, however, stimulation was recorded after 50  $\mu\text{mol}/\text{ml}$  of SCH and DHSB. This might indicate a different mechanism of AAPH effect on NO production.

#### Effects of silybin, silychristin and 2,3-dehydrosilybin on mitochondrial membrane potential

Next, we evaluated the effects of SB, SCH and DHSB on mitochondrial dynamics by measuring the mitochondrial membrane potential (MMP) referred to as  $\Delta\psi_m$  by flow cytometry. Values are expressed as mean fluorescence

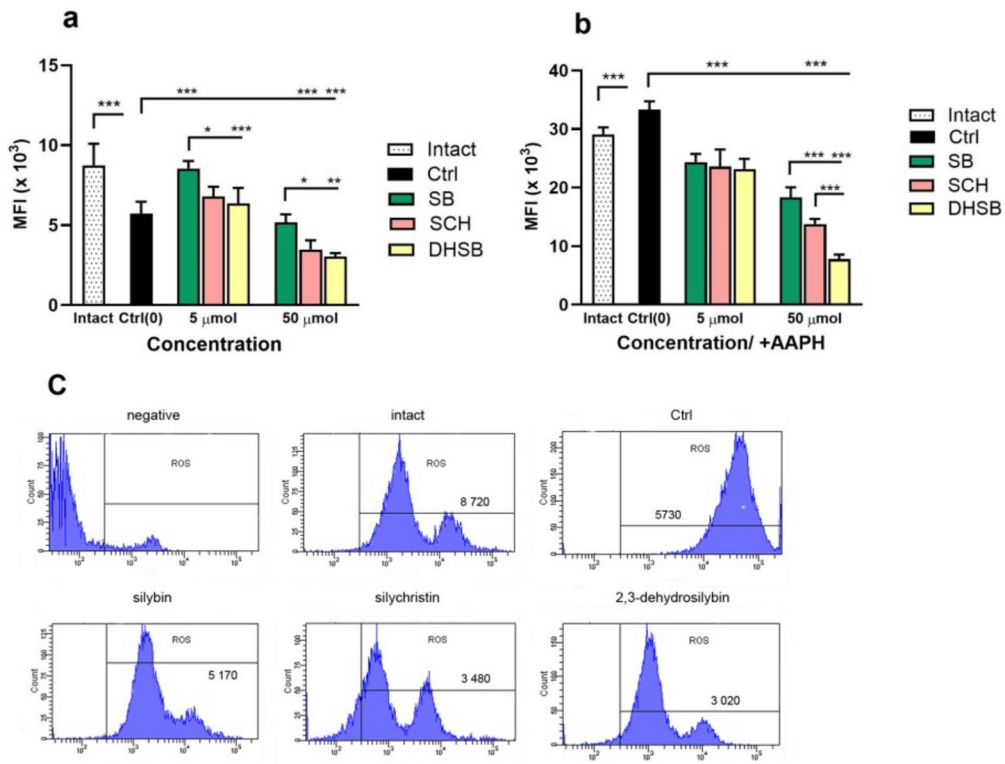


**Fig. 2.** Determination of intracellular ROS in intact cells, untreated control cells (Ctrl) and cells treated with 5 or 50  $\mu$ mol/ml of silybin (SB), silychristin (SCH), and 2,3-dehydrosilybin (DHSB) after 24 h incubation. AAPH was applied for last 1 h to induce oxidative stress. Values for ROS concentration shown on (a, b), are expressed as the mean fluorescence intensity/cell (MFI) (mean  $\pm$  SD, n=6). (c) Representative histograms for 50  $\mu$ mol/ml. Significantly different values between groups are indicated by lines and are marked as: \* $p$  < 0.05, \*\* $p$  < 0.01, \*\*\* $p$  < 0.001, ns—not significant.

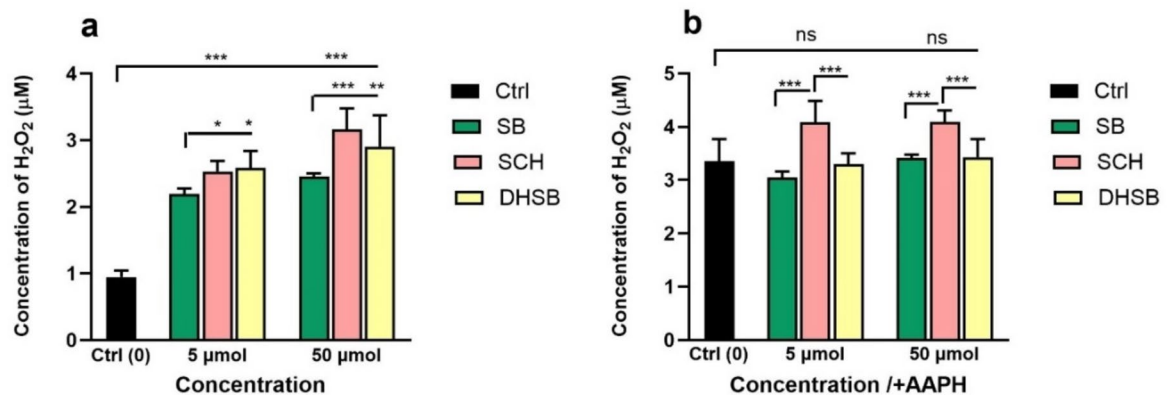


**Fig. 3.** Extracellular production of hydrogen peroxide by spleen cells after 2 h incubation in HBSS. Concentration was detected in cultures of control cells (Ctrl) and cells treated with 5 or 50  $\mu$ mol/ml of silybin (SB), silychristin (SCH), and 2,3-dehydrosilybin (DHSB) alone (**a**), or in combination with the oxidative stress inducer AAPH (**b**). Data are expressed in  $\mu$ M of  $H_2O_2$  and represent means  $\pm$  SD (n = 6). Significantly different values between groups indicated by lines are marked as: \* $p$  < 0.05, \*\* $p$  < 0.01, \*\*\* $p$  < 0.001, ns—not significant.

intensity/cell (MFI) (Fig. 5a,b) and representative histograms for selected groups are shown in Fig. 5c. Compared to freshly isolated cells, incubation for 24 h caused a significant decrease in  $\psi_m$  ( $p < 0.05$ ). The suppressive effect of cultivation was moderately alleviated after 5  $\mu\text{mol}/\text{ml}$  concentration, reaching values similar to those seen in the intact group. However, at 50  $\mu\text{mol}/\text{ml}$  concentration, all three compounds stimulated a significant activity of mitochondrial enzymes localized in the membranes, as reflected in the higher values of MFI in comparison with the control and the intact group. The stimulatory activity was in order DHSB > SB > SCH.

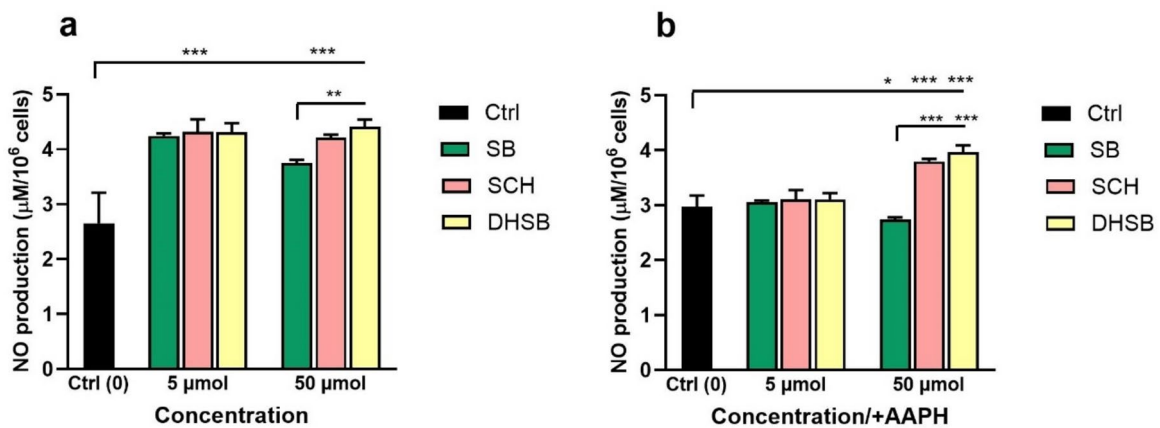


**Fig. 4.** Extracellular nitric oxide (NO) production by untreated control splenocytes (Ctrl) and cells treated with 5 or 50  $\mu\text{mol}/\text{ml}$  of silybin (SB), silychristin (SCH), and 2,3-dehydrosilybin (DHSB) (a), after 24 h incubation alone or in combination with AAPH (b). Data are expressed in  $\mu\text{M}$  of NO produced by  $1 \times 10^6$  cells/ml and represent means  $\pm$  SD ( $n=6$ ). Significantly different values between groups indicated by lines are marked as: \* $p < 0.05$ , \*\* $p < 0.01$ , \*\*\* $p < 0.001$ , ns—not significant.

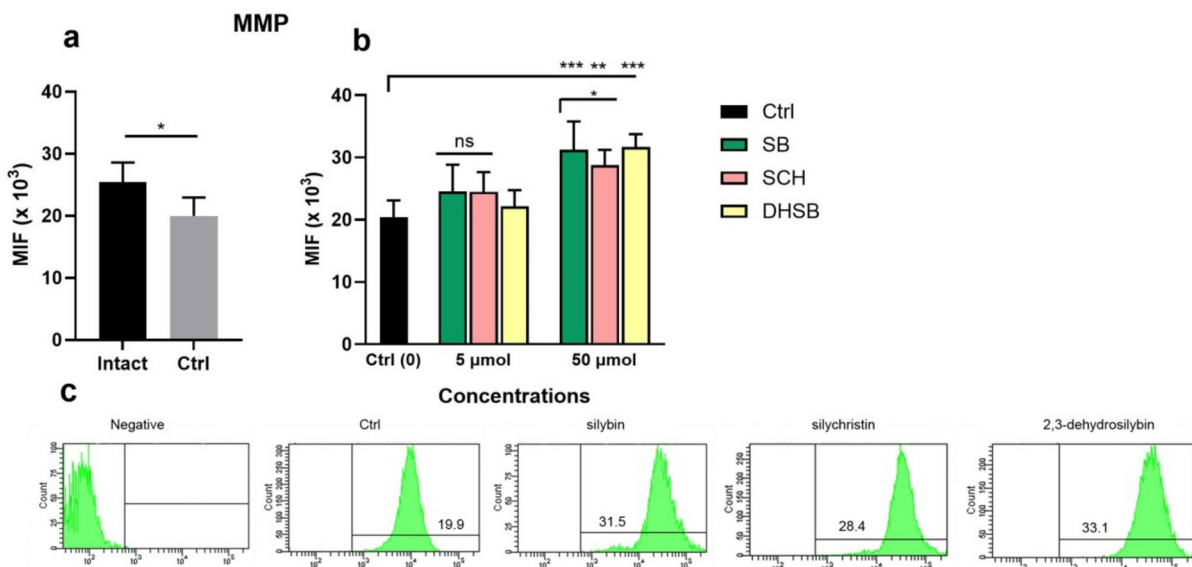


**Fig. 5.** Flow cytometric analysis of changes in mitochondrial membrane potential (MMP) referred as  $\Delta\psi_m$  are expressed as mean fluorescence intensity/cell (MFI) using rhodamine 123 as fluorescent dye. MMP was detected in intact splenocytes, control cells (Ctrl) and cells treated with 5 or 50  $\mu\text{mol}/\text{ml}$  of silybin (SB), silychristin (SCH), and 2,3-dehydrosilybin (DHSB) after 24 h incubation (a, b). (c) Representative histograms for 50  $\mu\text{mol}/\text{ml}$ . Values represent means  $\pm$  SD ( $n=6$ ). Significantly different values between groups indicated by lines are marked as: \* $p < 0.05$ , \*\* $p < 0.01$ , \*\*\* $p < 0.001$ , ns—not significant.

### Effects of silybin, silychristin and 2,3-dehydrosilybin on apoptosis

The effects of SB, SCH and DHSB at the concentrations of 5 and 50  $\mu\text{mol}/\text{ml}$  were also evaluated on the percentage of living cells, cells in the early stage of apoptosis, and in the late stage of apoptosis, including dead cells, by flow cytometry. In our spleen samples, the majority of freshly isolated splenocytes were alive ( $96.73 \pm 0.8\%$ ), and  $3.72 \pm 1.1\%$  were in the early stage of apoptosis. After 24 h incubation, only  $32.77 \pm 1.8\%$  were alive and up to  $61.98 \pm 2.1\%$  were already in the early stage of apoptosis (Fig. 6a). Treatment with both concentrations of compounds increased the proportions of live splenocytes ( $p < 0.001$ ) (Fig. 6b), and silybin was the most active ( $65.72 \pm 5.4\%$  and  $70.81 \pm 4.71\%$ , resp.). The second most protective was DHSB ( $64.07 \pm 3.6\%$  and  $67.22 \pm 1.86\%$ , resp.). Treatment with flavonolignans at both concentrations seemed to protect cells from entering into the early stage of apoptosis ( $p < 0.001$ ), showing no significant differences among individual compounds (Fig. 6c). SB at 50  $\mu\text{mol}/\text{ml}$  was the most effective ( $25.5 \pm 5.4\%$ ). In agreement with the effects on viability, the lowest

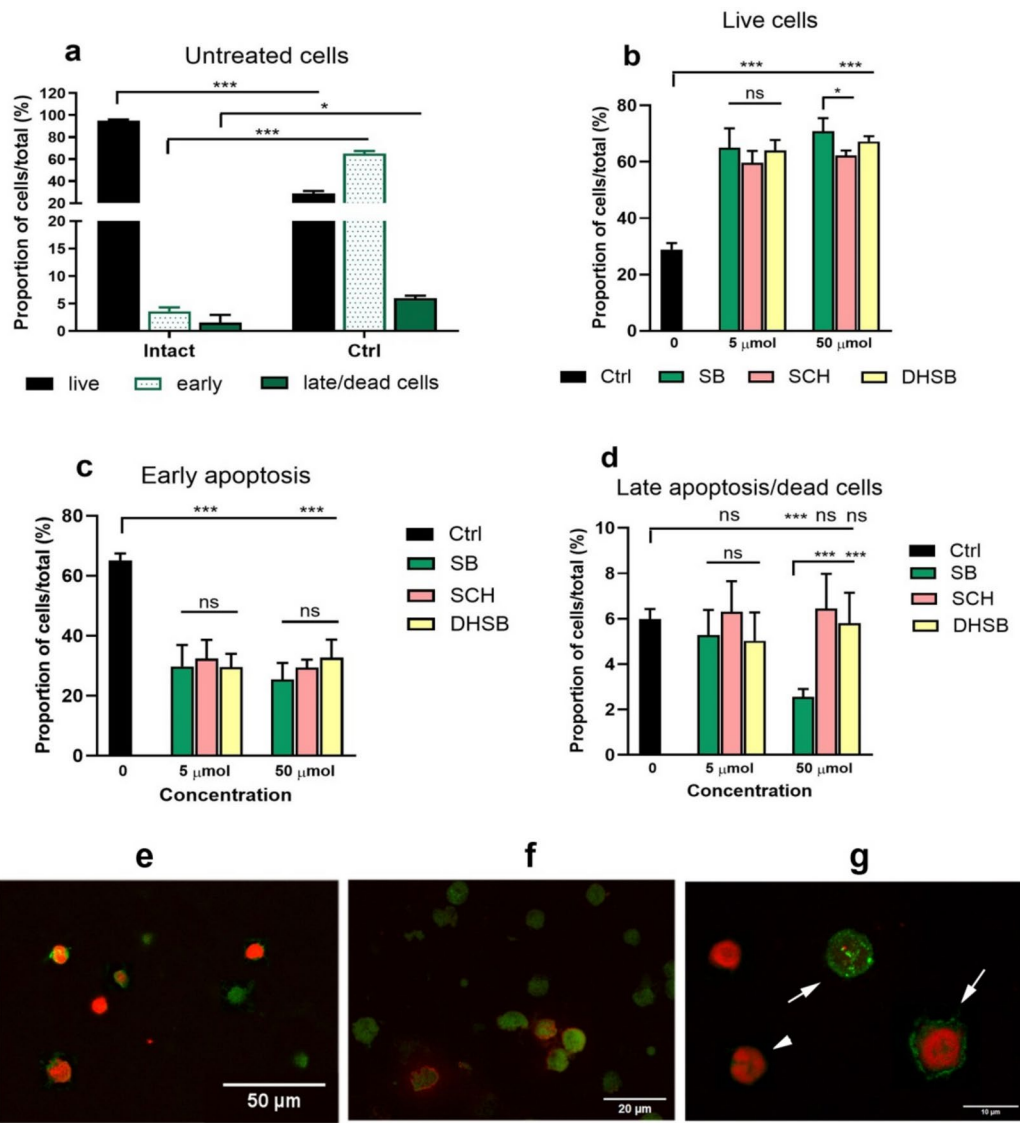


**Fig. 6.** Apoptosis in splenocytes, (a-d). Flow cytometric analysis of the proportions of live spleen cells, cells in the early stage and the late stage of apoptosis (including dead cells) after Annexin V and propidium iodide staining. Assay was performed on (a), intact cells, control cells (Ctrl) after 24 h incubation and cells treated with (b-d), silybin (SB), silychristin (SCH) and 2,3-dehydrosilybin (DHSB) at the concentrations of 5 or 50  $\mu$ mol/ml. Values represent means  $\pm$  SD (n = 6). Significantly different values between groups indicated by lines are marked as: \* $p$  < 0.05, \*\* $p$  < 0.001, ns—not significant. (e-g) Representative images of immunofluorescent localisation of Bcl-xL protein in splenocytes in (e), control group and cells treated with (f), SB and (g), DHSB (both at 50  $\mu$ mol/ml), showing differential immunoreactivity (arrows) (green colour) and nuclei (red colour). Arrowhead marks dying cell with fragmented nucleus.

numbers of dead cells were recorded at 50  $\mu$ mol/ml concentration of SB (2.55  $\pm$  0.3%) (Fig. 6d). Besides the flow cytometric analysis of apoptosis, the preliminary immunofluorescent detection of anti-apoptotic protein Bcl-xL was carried on. Representative microphotographs show the differential or missing immunoreactivity of the protein in splenocyte pools in the control group (Fig. 6e). Differential higher immunoreactivity was seen in cells treated with silybin (Fig. 6f) and 2,3-dehydrosilybin (Fig. 6g) (both at 50  $\mu$ mol/ml). Images show splenocytes in the individual stages of apoptosis and dead cells, indicating a cytoprotective effect of flavonolignans.

#### Effects of silybin, silychristin and 2,3-dehydrosilybin on the mRNA levels of genes regulating antioxidant pathways

The first line of defence against oxidative stress is provided by three protein antioxidants with enzymatic activity—*SOD1*, catalase (CAT) and glutathione peroxidase (GPx), which reduce ROS and hydrogen peroxide levels. The primary regulator of cell resistance to oxidative stress is the transcription factor nuclear factor erythroid 2-related factor 2 (*Nrf2*), which controls the basal and induced expression of a number of antioxidant defence genes. The mRNA levels were examined, to determine whether SB, SCH and DHSB at concentrations of

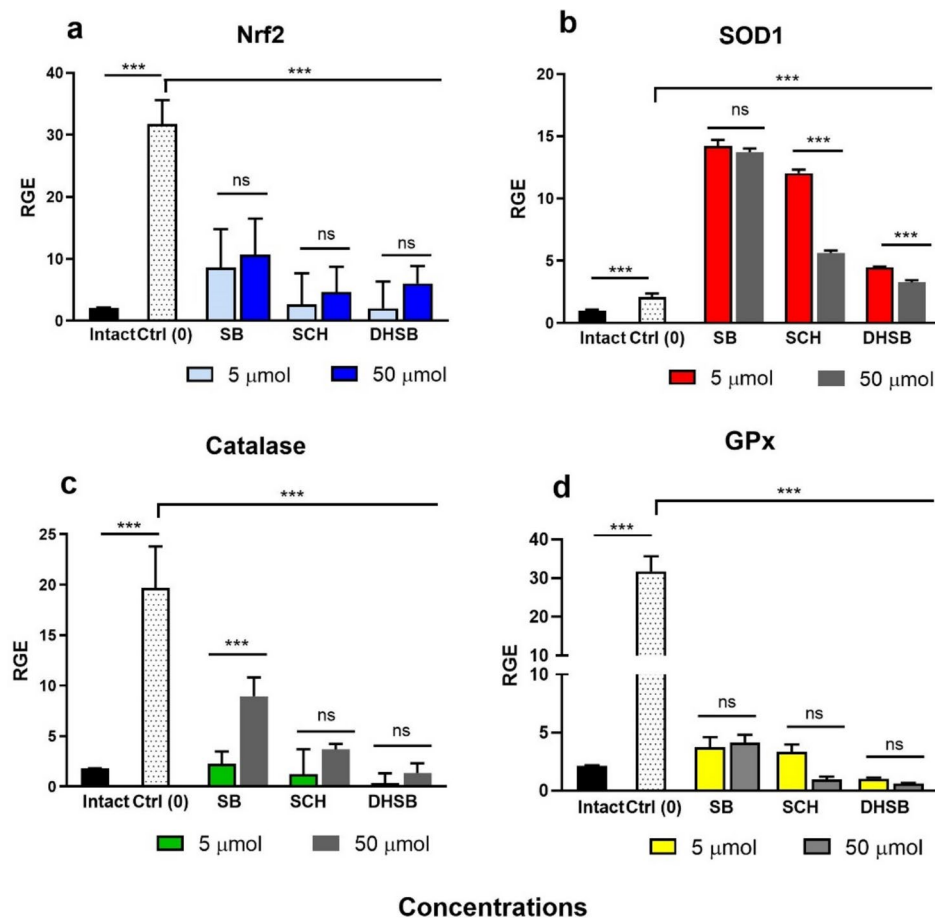


**Fig. 7.** Relative gene expression of antioxidant genes (a–d) *Nrf2*, *SOD1*, *CAT* and *GPx* analysed by real-time PCR in control cells (Ctrl) and cells treated with 5 or 50 μmol/ml of silybin (SB), silychristin (SCH), and 2,3-dehydrosilybin (DHSB) after 24 h incubation. Data (Ct values,  $n=6$ ) were normalised to housekeeping gene (*GAPDH*) and relative gene expression was calculated using the  $2^{-\Delta\Delta Ct}$  method using intact cell data as a calibration value. Significantly different values between groups indicated by lines are marked as: \*\*\* $p < 0.001$ , ns – not significant.

5 and 50 μmol/ml can modulate the activity of these antioxidant enzymes and transcription factors. Splenocytes underwent significant physiological changes already after 24 h of cultivation, as evidenced by a significant ( $p < 0.001$ ) increase of *Nrf2*, *SOD1*, *CAT* and *GPx* mRNA transcripts (Fig. 7a–d) compared to intact cells. Treatment of cells with the compounds at both concentrations reduced expression of *Nrf2* ( $p < 0.001$ ) (Fig. 7a), especially after SCH. By contrast, a marked increase of mRNA levels of *SOD1* ( $p < 0.001$ ) was detected, most pronounced after treatment with SB and SCH (Fig. 7b). In comparison with control, gene expression for *CAT* and *GPx* was significantly suppressed after treatment with all three compounds ( $p < 0.001$ ) (Fig. 7c,d), whereas only higher concentration of SB was slightly less suppressive on *CAT* activity than other compounds (Fig. 7c).

## Discussion

Spleen cells represent very sensitive primary cells suitable for studying the mechanisms by which natural substances can affect oxidative stress and related physiological processes. In our healthy Balb/c mice, they comprise approximately 80–85% of T and B lymphocytes and 15–20% of myeloid cells (dendritic cells and macrophages)<sup>25</sup>.

Under the standard culture conditions, atmospheric O<sub>2</sub> is unregulated and equilibrates in a CO<sub>2</sub> incubator at ~19–21% and does not ensure physiological conditions that occur *in vivo*. The organs and tissues of eukaryotic organisms require specific extracellular oxygen concentrations (1–11% O<sub>2</sub>), which characterize their own physioxia status<sup>19,27</sup>. We and others have demonstrated<sup>19,25,28–30</sup> that cultivation of different cell types under these standard conditions representing “hyperoxia” can negatively affect cell physiology, redox homeostasis, gene expression, cellular respiration and mitochondrial dynamics. In our study, cultivation of freshly isolated splenocytes for 24 h decreased splenocyte viability and metabolic activity as evaluated by MTT, Trypan blue exclusion test and neutral red uptake test, probably as a result of the oxidative stress due to hyperoxic conditions in the cell culture. The addition of flavonolignans (SB, SCH and DHSB) to splenocytes seemed to protect cells from the above-mentioned changes and cell death. The higher concentration (50 μmol/ml) had a significantly

more positive effect on cell metabolism and viability and SB was the most effective. The cytoprotective activity of SB, SCH and DHSB involves several mechanisms that relate to various cellular processes, of which the antioxidant and radical-scavenging activity is the most effective<sup>15,31</sup>. Similarly, using human keratinocyte and mouse fibroblast cell lines, Svobodová et al.<sup>32</sup> showed in the MTT assay that pre-treatment with SB and DHSB at 50  $\mu\text{mol}/\text{ml}$  decreased oxidative injury induced by hydrogen-peroxide applied in mmol concentrations significantly.

Due to the lack of information on how these compounds affect respiration and ROS production in splenocytes under standard conditions, we subsequently investigated the antioxidant capacity of SB, SCH and DHSB by measuring the production of intracellular ROS. The concentration of 50  $\mu\text{mol}/\text{ml}$  significantly reduced ROS levels in the cells, with DHSB being the most potent, also in the cell cultures in which oxidative stress was stimulated by AAPH. The weaker ability of SB in comparison with DHSB and SCH to scavenge both chemically generated superoxide and DPPH radicals was reported<sup>33,34</sup>. Authors showed that DHSB is more lipophilic and less water-soluble than SB, which predetermines it for an application in the lipophilic milieu, for example, as a cell membrane antioxidant. Numerous studies have shown that reactive oxygen species act as important physiological regulators of intracellular signaling pathways, activating or deactivating various receptors, proteins, and ions<sup>35–37</sup> and flavonolignans could interfere with mitochondrial and possibly other ROS-producing enzymes and transcription factors that regulate ROS level. The antioxidant enzyme *SOD1* maintains a low superoxide equilibrium state during oxidative stress in the cells by converting superoxide anion to  $\text{H}_2\text{O}_2$ <sup>38</sup>. Oxygen levels experienced by cells in the culture also influence hydrogen peroxide production via NADPH oxidase 1/4, highlighting the importance of regulating oxygen levels in the culture close to physiological values<sup>39</sup>. Compared to control cells,  $\text{H}_2\text{O}_2$  concentration after 2 h of incubation increased after treatment in the order SCH > DHSB > SB, and the higher levels of  $\text{H}_2\text{O}_2$  were seen after the higher concentrations of substances. We assume that apart from direct ROS scavenging activity, the conversion of ROS to  $\text{H}_2\text{O}_2$  occurred due to stimulation of *SOD1* enzyme. Unlike superoxide,  $\text{H}_2\text{O}_2$  can easily pass through the cell membrane into the extracellular space and may be present in low concentrations inside the cells. It appears that the increased levels of  $\text{H}_2\text{O}_2$  would not have negative effects, as at low concentrations it acts as an important signaling molecule<sup>40</sup>. SB and its derivatives significantly reduced  $\text{O}_2^-$  release and  $\text{H}_2\text{O}_2$  formation in PMA-stimulated monocytes, suggesting their specific activities in naïve versus inflammatory immune cells<sup>41</sup>.

Oxidative stress resulting from hyperoxia also negatively influences the mitochondrial functions<sup>42</sup>. The suppressive effect of culture conditions on  $\Delta\psi\text{m}$  was reversed and even increased above values in intact cells at 50  $\mu\text{mol}/\text{ml}$  concentration in order DHSB > SB > SCH. This effect could be the result of their different antioxidant capacity<sup>15</sup>. As the elevation of  $\Delta\psi\text{m}$  above the values in intact cells correlates with stimulation of viability in MTT assay, flavonolignans probably protected enzymes localized in the mitochondrial membranes and NADH/NADPH in the cells. It was documented that SB and SCH at the concentration up to 100  $\mu\text{mol}/\text{ml}$  did not have a cytotoxic effect on PBMC and platelets, increased mitochondrial membrane potential and protected cellular mitochondria<sup>43</sup>.

Numerous studies showed that apoptosis is tightly associated with changes in  $\Delta\psi\text{m}$ , and the decline of ATP generation below threshold value leads to mitochondrial dysfunction and initiation of diseases<sup>44,45</sup>. Apoptosis can be defined by a series of biochemical and morphological changes, including an increase in ROS level, activation of caspases, cell shrinkage, chromatin condensation and nucleosomal degradation<sup>46,47</sup>. In agreement with our previous data, 24 h cultivation resulted in the transition of about 60% of splenocytes to the early stage of apoptosis. Treatment with all three flavonolignans, already at low concentration, prevented the changes in mitochondrial membrane potential and probably in other compartments, resulting in an increased population of live splenocytes. These data are consistent with the observed effects on viability, cytotoxicity and metabolic activity. SB had anti-apoptotic activity, stimulated metabolic viability as well as proliferation in a normal intestinal cell line (IPEC-1), but showed higher cytotoxic, antiproliferative and anti-inflammatory activities in the CaCo cancer cell line<sup>48</sup>. The antiapoptotic activity of SB, SCH and DHSB on primary immune cells and normal cell lines contrasts with the induction of apoptosis in various cancer cell lines in vitro and in vivo<sup>49,50</sup>.

SCH is the second most abundant flavonolignan in silymarin extract. Its strong antioxidant activities were proved by biochemical DPPH and ABTS radical scavenging assays, in which antioxidant activity of SCH was nearly 14× higher than that of SB and about 1.5 times lower than DHSB<sup>51</sup>. Compared to other flavonolignans, less is known about its biological activities. In the present study, we observed the slightly weaker sensitivity of primary mouse splenocytes to their cytoprotective and antiapoptotic effects in comparison with SB and DHSB.

Nitric oxide (NO) is produced inside the mitochondria by mitochondrial nitric oxide synthase<sup>52</sup> and also diffuses into the mitochondria from the cytosol. In our study, the NO concentrations in the cells treated with SB, SCH and DHSB (5 and 50  $\mu\text{mol}/\text{ml}$ ) increased significantly compared to the control, while the lower concentration stimulated the production of NO more than the higher one. ROS such as  $\text{O}_2^-$  and  $\text{H}_2\text{O}_2$  can directly or indirectly activate redox-sensitive transcriptional factor NF- $\kappa\text{B}$  that is involved in the expression of pro-inflammatory genes including inducible nitric oxide synthase (iNOS)<sup>53</sup> which is responsible for synthesis of NO. Free radicals themselves can also modulate the function of iNOS<sup>54</sup>. The increased levels of NO after treatment with SB, SCH and DHSB correlated with elevated concentration of  $\text{H}_2\text{O}_2$  in treated groups in agreement with the study of Wang et al.<sup>55</sup> who observed moderately elevated NO levels and iNOS expression after 50  $\mu\text{M}$  concentration of SB in MCF-7 cancer cell line. The opposite inhibitory effect on NO production after SB and DHSB treatment for 48 h was reported in LPS- stimulated RAW264 macrophage cell line indicating the anti-inflammatory effect<sup>16</sup>. As NO is a weak oxidant, we suppose that the redox scavenging activity of flavonolignans probably prevented the reaction of  $\text{O}_2^-$  with NO forming dangerous oxidant peroxynitrite ( $\text{ONOO}^-$ ) in correlation with cytoprotective and anti-apoptotic effect in unstimulated splenocytes. The excess of  $\text{H}_2\text{O}_2$  is converted to water and molecular oxygen  $\text{O}_2$  by the antioxidant enzyme catalase (CAT)<sup>56</sup> and glutathione peroxidase (GPx)<sup>57</sup>, which are present in almost all aerobic organisms. *Nrf2* is ubiquitously and constitutively expressed by cells, providing a prompt

protective response to oxidative, inflammatory, and metabolic stresses<sup>58,59</sup>. Compared to the intact cells, increased mRNA transcription of *Nrf2*, *SOD1*, *CAT* and *GPx* genes was observed in the control group. Treatment of the cells with flavonolignans reduced mRNA copies for *Nrf2* at both monitored concentrations compared to the control. Downregulation of *Nrf2* transcription seems to be directly linked to the reduction of oxidative and metabolic stress<sup>58</sup>. Conversely, flavonolignans significantly stimulated the expression of *SOD1* compared to the control, which is in correlation with increased conversion of ROS to H<sub>2</sub>O<sub>2</sub>. Gene transcription was strongly downregulated compared to control in order DHSB > SCH > SB. The data imply that the transcriptional activity of these antioxidant genes in splenocytes is regulated by ROS concentrations and reflects the specific antioxidant capacity of individual flavonolignans.

## Conclusion

Cultivation under standard conditions with the access of atmospheric oxygen to the medium probably induced hyperoxia, which in turn led to splenocytes responding to moderate oxidative stress with decreased viability, pro-apoptotic changes and disruption of the redox balance. A cytoprotective effect was observed for SB, SCH and DHSB at a concentration of 5 µmol/ml, with a concentration of 50 µmol/ml appearing to renew and stimulate the hyperoxia-induced decrease in physiological functions, in the order SB > DHSB > SCH. The concentration-dependent effect of the substances in restoring the redox balance based on the concentration of ROS, H<sub>2</sub>O<sub>2</sub> and NO was found in the order DHSB > SCH > SB. This may be correlated with the suppression of *Nrf2*, *CAT* and *GPx* gene expression. The strong stimulation of the *SOD1* gene may indicate its dominant role in inducing redox homeostasis during oxidative stress caused by oxygen radicals, and the capacity of flavonolignans to stimulate its gene expression during oxidative stress.

## Data availability

All data generated or analysed during this study are included in this article and its supplementary information file. Primer sequences are provided in Supplementary Table 1, along with original reference describing the sequences used in this study.

Received: 10 July 2024; Accepted: 7 February 2025

Published online: 15 February 2025

## References

- Petraskova, L., Kanova, K., Biedermann, D., Kren, V. & Valentova, K. Simple and rapid HPLC separation and quantification of flavonoid, flavonolignans, and 2,3-dehydroflavonolignans in silymarin. *Foods* <https://doi.org/10.3390/Foods9020116> (2020).
- Tvrdy, V. et al. Systematic review of pharmacokinetics and potential pharmacokinetic interactions of flavonolignans from silymarin. *Med. Res. Rev.* **41**, 2195–2246. <https://doi.org/10.1002/med.21791> (2021).
- Gazák, R., Walterová, D. & Kren, V. Silybin and silymarin -: New and emerging applications in medicine. *Curr. Med. Chem.* **14**, 315–338. <https://doi.org/10.2174/092986707779941159> (2007).
- Kuo, F. H. & Jan, T. R. Silibinin attenuates antigen-specific IgE production through the modulation of Th1/Th2 balance in ovalbumin-sensitized BALB/c mice. *Phytomedicine* **16**, 271–276. <https://doi.org/10.1016/j.phymed.2008.07.006> (2009).
- Esmaili, N., Anaraki, S. B., Gharagozloo, M. & Moayedi, B. Silymarin impacts on immune system as an immunomodulator: One key for many locks. *Int. Immunopharmacol.* **50**, 194–201. <https://doi.org/10.1016/j.intimp.2017.06.030> (2017).
- Chambers, C. S. et al. The silymarin composition ... and why does it matter???. *Food Res. Int.* **100**, 339–353. <https://doi.org/10.1016/j.foodres.2017.07.017> (2017).
- Camini, F. C. & Costa, D. C. Silymarin: Not just another antioxidant. *J. Basic Clin. Physiol. Pharmacol.* <https://doi.org/10.1515/jbcpp-2019-0206> (2020).
- Gu, M. et al. Silymarin ameliorates metabolic dysfunction associated with diet-induced obesity via activation of farnesyl X receptor. *Front. Pharmacol.* **7**, 345. <https://doi.org/10.3389/fphar.2016.00345> (2016).
- Surai, P. F. Silymarin as a natural antioxidant: An overview of the current evidence and perspectives. *Antioxid. Basel.* **4**, 204–247. <https://doi.org/10.3390/antiox4010204> (2015).
- Oufi, H. G. & Al-Shawi, N. N. The effects of different doses of silibinin in combination with methotrexate on testicular tissue of mice. *Eur. J. Pharmacol.* **730**, 36–40. <https://doi.org/10.1016/j.ejphar.2014.02.010> (2014).
- Adhikari, M. & Arora, R. Nano-silymarin provides protection against  $\gamma$ -radiation-induced oxidative stress in cultured human embryonic kidney cells. *Mutat. Res. Genet. Toxicol. Environ. Mutagenesis.* **792**, 1–11. <https://doi.org/10.1016/j.mrgentox.2015.08.006> (2015).
- Svobodová, A. R. et al. UVA-photoprotective potential of silymarin and silybin. *Arch. Dermatol. Res.* **310**, 413–424. <https://doi.org/10.1007/s00403-018-1828-6> (2018).
- Qin, N. B. et al. Hypoglycemic effect of silychristin A from fruit via protecting pancreatic islet cells from oxidative damage and inhibiting  $\alpha$ -glucosidase activity and in rats with type 1 diabetes. *J. Funct. Foods* **38**, 168–179. <https://doi.org/10.1016/j.jff.2017.09.013> (2017).
- Bijak, M., Dziedzic, A., Synowiec, E., Sliwinski, T. & Saluk-Bijak, J. Flavonolignans Inhibit IL1- $\beta$ -induced cross-talk between blood platelets and leukocytes. *Nutrients* **9**, 1022. <https://doi.org/10.3390/Nu9091022> (2017).
- Gazák, R. et al. Molecular mechanisms of silybin and 2,3-dehydrosilybin antiradical activity–role of individual hydroxyl groups. *Free Radic. Biol. Med.* **46**, 745–758. <https://doi.org/10.1016/j.freeradbiomed.2008.11.016> (2009).
- Dobiasová, S. et al. Multidrug resistance modulation activity of silybin derivatives and their anti-inflammatory potential. *Antioxid. Basel.* **9**, 455. <https://doi.org/10.3390/Antiox9050455> (2020).
- Gillesen, A. & Schmidt, H. H. J. Silymarin as supportive treatment in liver diseases: A narrative review. *Adv. Therapy* **37**, 1279–1301. <https://doi.org/10.1007/s12325-020-01251-y> (2020).
- Cemerski, S., Van Meerwijk, J. P. & Romagnoli, P. Oxidative-stress-induced T lymphocyte hyporesponsiveness is caused by structural modification rather than proteasomal degradation of crucial TCR signaling molecules. *Eur. J. Immunol.* **33**, 2178–2185. <https://doi.org/10.1002/eji.200323898> (2003).
- Alva, R., Gardner, G. L., Liang, P. & Stuart, J. A. Supraphysiological oxygen levels in mammalian cell culture: Current state and future perspectives. *Cells* **11**, 3123. <https://doi.org/10.3390/Cells11193123> (2022).
- Krenek, K., Marhol, P., Peikerová, Z., Kren, V. & Biedermann, D. Preparatory separation of the silymarin flavonolignans by Sephadex LH-20 gel. *Food Res. Int.* **65**, 115–120. <https://doi.org/10.1016/j.foodres.2014.02.001> (2014).

21. Maitrejean, M. et al. The flavanolignan silybin and its hemisynthetic derivatives, a novel series of potential modulators of P-glycoprotein. *Bioorg. Med. Chem. Lett.* **10**, 157–160. [https://doi.org/10.1016/s0960-894x\(99\)00636-8](https://doi.org/10.1016/s0960-894x(99)00636-8) (2000).
22. Repetto, G., Del Peso, A. & Zurita, J. L. Neutral red uptake assay for the estimation of cell viability/cytotoxicity. *Nat. Protoc.* **3**, 1125–1131. <https://doi.org/10.1038/nprot.2008.75> (2008).
23. Tirichen, H. et al. Mitochondrial reactive oxygen species and their contribution in chronic kidney disease progression through oxidative stress. *Front. Physiol.* **12**, 627837. <https://doi.org/10.3389/fphys.2021.627837> (2021).
24. Santos, L. C., Honda, N. K., Carlos, I. Z. & Vilegas, W. Intermediate reactive oxygen and nitrogen from macrophages induced by Brazilian lichens. *Fitoterapia* **75**, 473–479. <https://doi.org/10.1016/j.fitote.2004.04.002> (2004).
25. Jurčáková, Z. et al. Astaxanthin extract from and its fractions of astaxanthin mono- and diesters obtained by CCC show differential antioxidant and cytoprotective effects on naive-mouse spleen cells. *Antioxid. Basel* **12**, 1144. <https://doi.org/10.3390/Antiox12061144> (2023).
26. Livak, K. J. & Schmittgen, T. D. Analysis of relative gene expression data using real-time quantitative PCR and the  $2^{-\Delta\Delta CT}$  method. *Methods* **25**, 402–408. <https://doi.org/10.1006/meth.2001.1262> (2001).
27. Carreau, A., El Hafny-Rahbi, B., Matejuk, A., Grillon, C. & Kieda, C. Why is the partial oxygen pressure of human tissues a crucial parameter? Small molecules and hypoxia. *J. Cell Mol. Med.* **15**, 1239–1253. <https://doi.org/10.1111/j.1582-4934.2011.01258.x> (2011).
28. Fonseca, J., Moradi, F., Valente, A. J. E. & Stuart, J. A. Oxygen and glucose levels in cell culture media determine resveratrol's effects on growth, hydrogen peroxide production, and mitochondrial dynamics. *Antioxid. Basel* **7**, 157. <https://doi.org/10.3390/Antiox710157> (2018).
29. Moradi, F., Moffatt, C. & Stuart, J. A. The effect of oxygen and micronutrient composition of cell growth media on cancer cell bioenergetics and mitochondrial networks. *Biomolecules* <https://doi.org/10.3390/biom11081177> (2021).
30. Alva, R. et al. Oxygen toxicity: Cellular mechanisms in normobaric hyperoxia. *Cell Biol. Toxicol.* **39**, 111–143. <https://doi.org/10.1007/s10565-022-09737-7> (2023).
31. Valenzuela, A. & Garrido, A. Biochemical bases of the pharmacological action of the flavonoid silymarin and of its structural isomer silibinin. *Biol. Res.* **27**, 105–112 (1994).
32. Svbodová, A., Walterová, D. & Psotová, J. Influence of silymarin and its flavonolignans on  $H_2O_2$ -induced oxidative stress in human keratinocytes and mouse fibroblasts. *Burns* **32**, 973–979. <https://doi.org/10.1016/j.burns.2006.04.004> (2006).
33. Trouillas, P. et al. Mechanism of the antioxidant action of silybin and 2,3-dehydrosilybin flavonolignans: A joint experimental and theoretical study. *J. Phys. Chem. A* **112**, 1054–1063. <https://doi.org/10.1021/jp075814h> (2008).
34. Anthony, K. P. & Saleh, M. A. Free radical scavenging and antioxidant activities of silymarin components. *Antioxid. Basel* **2**, 398–407. <https://doi.org/10.3390/antiox2040398> (2013).
35. Finkel, T. Signal transduction by reactive oxygen species. *J. Cell Biol.* **194**, 7–15. <https://doi.org/10.1083/jcb.201102095> (2011).
36. Kaulmann, A. & Bohn, T. Carotenoids, inflammation, and oxidative stress-implications of cellular signaling pathways and relation to chronic disease prevention. *Nutr. Res.* **34**, 907–929. <https://doi.org/10.1016/j.nutres.2014.07.010> (2014).
37. Zhang, J. X. et al. ROS and ROS-mediated cellular signalling. *Oxid. Med. Cell. Longev.* **2016**, 4350965. <https://doi.org/10.1155/2016/4350965> (2016).
38. Juarez, J. C. et al. Superoxide dismutase 1 (SOD1) is essential for  $H_2O_2$ -mediated oxidation and inactivation of phosphatases in growth factor signaling. *Proc. Natl. Acad. Sci. U. S. A.* **105**, 7147–7152. <https://doi.org/10.1073/pnas.0709451105> (2008).
39. Maddalena, L. A. et al. Hydrogen peroxide production is affected by oxygen levels in mammalian cell culture. *Biochem. Biophys. Res. Commun.* **493**, 246–251. <https://doi.org/10.1016/j.bbrc.2017.09.037> (2017).
40. Liochev, S. I. Reactive oxygen species and the free radical theory of aging. *Free Radical Bio Med.* **60**, 1–4. <https://doi.org/10.1016/j.freeradbiomed.2013.02.011> (2013).
41. Tan, H. Y. et al. The reactive oxygen species in macrophage polarization: Reflecting its dual role in progression and treatment of human diseases. *Oxid. Med. Cell Longev.* **2016**, 2795090. <https://doi.org/10.1155/2016/2795090> (2016).
42. Guo, C. Y., Sun, L., Chen, X. P. & Zhang, D. S. Oxidative stress, mitochondrial damage and neurodegenerative diseases. *Neural Regener. Res.* **8**, 2003–2014. <https://doi.org/10.3969/j.issn.1673-5374.2013.21.009> (2013).
43. Bijak, M., Synowiec, E., Sitarek, P., Sliwinski, T. & Saluk-Bijak, J. Evaluation of the cytotoxicity and genotoxicity of flavonolignans in different cellular models. *Nutrients* **9**, 1356. <https://doi.org/10.3390/Nu9121356> (2017).
44. Ly, J. D., Grubb, D. R. & Lawen, A. The mitochondrial membrane potential ( $\Delta\psi_m$ ) in apoptosis: An update. *Apoptosis* **8**, 115–128. <https://doi.org/10.1023/A:1022945107762> (2003).
45. Zorova, L. D. et al. Mitochondrial membrane potential. *Anal. Biochem.* **552**, 50–59. <https://doi.org/10.1016/j.ab.2017.07.009> (2018).
46. Vander Heiden, M. G., Chandel, N. S., Williamson, E. K., Schumacker, P. T. & Thompson, C. B. Bcl-xL regulates the membrane potential and volume homeostasis of mitochondria. *Cell* **91**, 627–37. [https://doi.org/10.1016/s0092-8674\(00\)80450-x](https://doi.org/10.1016/s0092-8674(00)80450-x) (1997).
47. Simon, H. U., Haj-Yehia, A. & Levi-Schaffer, F. Role of reactive oxygen species (ROS) in apoptosis induction. *Apoptosis* **5**, 415–418. <https://doi.org/10.1023/a:1009616228304> (2000).
48. Faixová, D. et al. Silybin showed higher cytotoxic, antiproliferative, and anti-inflammatory activities in the CaCo cancer cell line while retaining viability and proliferation in normal intestinal IPEC-1 cells. *Life-Basel* **13**, 492. <https://doi.org/10.3390/Life13020492> (2023).
49. Tilley, C. et al. Silibinin and its 2,3-dehydro-derivative inhibit basal cell carcinoma growth via suppression of mitogenic signaling and transcription factors activation. *Mol. Carcinog.* **55**, 3–14. <https://doi.org/10.1002/mc.22253> (2016).
50. Deep, G. et al. Silibinin inhibits hypoxia-induced HIF-1alpha-mediated signaling, angiogenesis and lipogenesis in prostate cancer cells: In vitro evidence and in vivo functional imaging and metabolomics. *Mol. Carcinog.* **56**, 833–848. <https://doi.org/10.1002/mc.22537> (2017).
51. Biedermann, D. et al. Silychristin: Skeletal alterations and biological activities. *J. Nat. Prod.* **79**, 3086–3092. <https://doi.org/10.1021/acs.jnatprod.6b00750> (2016).
52. Carreras, M. C., Franco, M. C., Peralta, J. G. & Poderoso, J. J. Nitric oxide, complex I, and the modulation of mitochondrial reactive species in biology and disease. *Mol. Aspects Med.* **25**, 125–139. <https://doi.org/10.1016/j.mam.2004.02.014> (2004).
53. Flohé, L., Brigelius-Flohé, R., Saliou, C., Traber, M. G. & Packer, L. Redox regulation of NF-kappa B activation. *Free Radical Bio Med.* **22**, 1115–1126. [https://doi.org/10.1016/S0891-5849\(96\)00501-1](https://doi.org/10.1016/S0891-5849(96)00501-1) (1997).
54. Ritchie, R. H., Drummond, G. R., Sobey, C. G., De Silva, T. M. & Kemp-Harper, B. K. The opposing roles of NO and oxidative stress in cardiovascular disease. *Pharmacol. Res.* **116**, 57–69. <https://doi.org/10.1016/j.phrs.2016.12.017> (2017).
55. Wang, H. J. et al. Silibinin induces the generation of nitric oxide in human breast cancer MCF-7 cells. *Free Radic. Res.* **44**, 577–584. <https://doi.org/10.3109/10715761003692495> (2010).
56. Nandi, A., Yan, L. J., Jana, C. K. & Das, N. Role of catalase in oxidative stress- and age-associated degenerative diseases. *Oxid. Med. Cell. Longev.* **2019**, 9613090. <https://doi.org/10.1155/2019/9613090> (2019).
57. Pei, J., Pan, X. Y., Wei, G. H. & Hua, Y. Research progress of glutathione peroxidase family (GPX) in redox regulation. *Front. Pharmacol.* **14**, 1147414. <https://doi.org/10.3389/fphar.2023.1147414> (2023).
58. Tonelli, C., Chio, I. I. C. & Tuveson, D. A. Transcriptional regulation by Nrf2. *Antioxid. Redox Signal.* **29**, 1727–1745. <https://doi.org/10.1089/ars.2017.7342> (2018).
59. Robledinos-Antón, N., Fernández-Ginés, R., Manda, G. & Cuadrado, A. Activators and inhibitors of NRF2: A review of their potential for clinical development. *Oxid. Med. Cellul. Longev.* **2019**, 9372182. <https://doi.org/10.1155/2019/9372182> (2019).

## Acknowledgements

This study was funded by the Scientific Grant Agency of the Ministry of Education of the Slovak Republic and the Slovak Academy of Sciences, grant number VEGA 2/0033/21, grant number APVV—17-0410 and international project funded by the European Union—the COST Action no. CA21111 “One Health drugs against parasitic vector borne diseases in Europe and beyond” (OneHealthdrugs)/MVTs (Slovak Republic).

## Author contributions

ZJ: conceptualization, methodology, investigation, data curation, writing; GH: conceptualization, methodology, investigation, data curation, writing, and review, funding acquisition; DM: methodology, data curation; AAM: methodology, data curation; DB: methodology, writing.

## Declarations

### Competing interests

The authors declare no competing interests.

### Additional information

**Supplementary Information** The online version contains supplementary material available at <https://doi.org/10.1038/s41598-025-89824-1>.

**Correspondence** and requests for materials should be addressed to G.H.

**Reprints and permissions information** is available at [www.nature.com/reprints](http://www.nature.com/reprints).

**Publisher's note** Springer Nature remains neutral with regard to jurisdictional claims in published maps and institutional affiliations.

**Open Access** This article is licensed under a Creative Commons Attribution-NonCommercial-NoDerivatives 4.0 International License, which permits any non-commercial use, sharing, distribution and reproduction in any medium or format, as long as you give appropriate credit to the original author(s) and the source, provide a link to the Creative Commons licence, and indicate if you modified the licensed material. You do not have permission under this licence to share adapted material derived from this article or parts of it. The images or other third party material in this article are included in the article's Creative Commons licence, unless indicated otherwise in a credit line to the material. If material is not included in the article's Creative Commons licence and your intended use is not permitted by statutory regulation or exceeds the permitted use, you will need to obtain permission directly from the copyright holder. To view a copy of this licence, visit <http://creativecommons.org/licenses/by-nc-nd/4.0/>.

© The Author(s) 2025